



Norwegian
Meteorological Institute
met.no

met.no report

no. 17/2009
Oceanography

Iceberg modeling at met.no: Validation of iceberg model

Göran Broström, Arne Melsom
Norwegian Meteorological Institute

Mohamed Sayed, Ivana Kubat
Canadian Hydraulics Center

Title

Iceberg modeling at met.no: Validation of iceberg model

Section

Oceanography

Author(s)

Göran Broström

Arne Melsom

Mohamed Sayed

Ivana Kubat

Date

21122009

Report no.

17

Classification

Free Restricted

ISSN 1503-8025

e-ISSN <number>

Client's reference

Contract 4501431719

Client(s)

StatoilHydro

Abstract

The present study is a part of an effort to implement the Canadian Hydraulics Centre (CHC) iceberg model in the Norwegian Meteorological Institute (met.no) operational system. One important part of the implementation plan is to validate the system against observations. The validation is separated into two parts: i) a validation of the current model that is used to force the drift of the icebergs; this study is presented in an accompanying study (Broström et al., 2009); ii) the second part is to validate the iceberg drift using available observations of iceberg trajectories, the second validation study is presented here.

This report describes the met.no implementation of the iceberg drift and deterioration model developed at the Canadian Hydraulic Centre (CHC) (Kubat et al., 2007; Kubat et al., 2005). Furthermore, the iceberg model is validated against some observations on iceberg drift obtained spring 1988 during the Ice Data Acquisition Program (IDAP) (Spring, 1994). It is shown that the CHC iceberg model, forced with the met.no hindcast data for 1988, has good capability in reproducing the observed iceberg drift. It is proposed that the largest unknown for the present iceberg model validation exercise is the geometrical shape of the iceberg (i.e., type of iceberg and the horizontal and vertical length scales), and uncertainties in the ocean currents, ice movements, and wave forcing.

Keywords

Validation, ocean model, iceberg model

Disiplinary signature

Lars Petter Røed (sign)

Responsible signature

Øystein Hov (sign)

Executive summary

The present study is a part of an effort to implement the Canadian Hydraulics Centre (CHC) iceberg model in the Norwegian Meteorological Institute (met.no) operational system. One important part of the implementation plan is to validate the system against observations. The validation is separated into two parts: i) a validation of the current model that is used to force the drift of the icebergs; this study is presented in an accompanying study (Broström et al., 2009): ii) the second part is to validate the iceberg drift using available observations of iceberg trajectories, the second validation study is presented here.

This report describes the met.no implementation of the iceberg drift and deterioration model developed at the Canadian Hydraulic Centre (CHC) (Kubat et al., 2007; Kubat et al., 2005). Furthermore, the iceberg model is validated against some observations on iceberg drift obtained spring 1988 during the Ice Data Acquisition Program (IDAP) (Spring, 1994). It is shown that the CHC iceberg model, forced with the met.no hindcast data for 1988, has good capability in reproducing the observed iceberg drift. It is proposed that the largest unknown for the present iceberg model validation exercise is the geometrical shape of the iceberg (i.e., type of iceberg and the horizontal and vertical length scales), and uncertainties in the ocean currents, ice movements, and wave forcing.

List of content

EXECUTIVE SUMMARY	3
1 INTRODUCTION.....	5
1.1 REGIONAL DESCRIPTION.....	5
1.2 THE IDAP STUDY	6
1.3 AIM OF STUDY	11
2 ICEBERG MODEL	12
2.1 MOMENTUM BALANCE	12
2.2 DETERIORATION MODULE (OR MASS BALANCE)	14
2.2.1 Model description	15
3 VALIDATION OF THE ICEBERG MODEL	18
3.1 FORCING DATA	18
3.2 ICEBERG DRIFT	19
3.2.1 Experiments with different iceberg type and iceberg size.....	19
3.2.2 Experiments with various forcing	24
3.3 DEVIATION BETWEEN MODEL AND OBSERVATIONS	26
3.4 MODEL RESULTS USING ALL DATA	28
3.4 VELOCITY FREQUENCY.....	30
3.5 DETERIORATION.....	30
4 RESULTS AND DISCUSSION.....	32
4.1 POSSIBLE MODEL IMPROVEMENTS	32
REFERENCES.....	34

1 Introduction

Each year there are several icebergs in the Barents Sea. The icebergs pose a threat to shipping and off-shore industries and it is desirable to be able to forecast iceberg motions in the Barents Sea to increase safety of marine operations. Furthermore, it is valuable to have a model tool to investigate the statistical properties, such as iceberg distributions and iceberg sizes, in the Barents Sea for more accurate risk predictions regarding shipping and oil and gas exploration. The results from risk predictions may also be used for designing equipments to be used in Barents Sea.

As of today, the most comprehensive iceberg model is probably the model developed at the Canadian Hydraulics Center (CHC) (Kubat et al., 2007; Kubat et al., 2005), which is used operationally at the Canadian Ice Service (CIS) and the International Ice Patrol (IIP). A version of this model is also being used to determine iceberg movements in the vicinity of oil rigs at Grand Banks and provides a guide for decisions on the towing of icebergs. To increase the modeling capabilities for iceberg geometry and iceberg drift in the Barents Sea the present project aims to incorporate the CHC iceberg model into the operational system at met.no. Furthermore, another significant part of the project is to validate the iceberg model for 1987-1988: the underlying physical forcing is analyzed in an accomplishing report (Broström et al., 2009) while the iceberg model description and validation is presented here.

1.1 Regional description

The aim of the present model exercise is to validate the CHC iceberg model, *i.e.*, iceberg drift and dynamics, for the Barents Sea region. The icebergs in the Barents Sea mainly come from the Franz Josef Land, Svalbard, and Novaja Semlja (Spring, 1994): a map of the Barents Sea area showing some important glaciers producing icebergs for the Barents Sea area is given in Fig. 1.1. Icebergs are mainly transported by ocean currents and sea ice movements¹. The wave stresses on an iceberg is also an important factor for the iceberg drift albeit it is generally smaller than the impact of ocean currents and sea ice movements. Here it may be noted that sea ice may also be import for decreasing the wave amplitude (Broström & Christensen, 2008; Squire, 2007; Squire et al., 1995), which is an important factor for iceberg movements and deterioration. For iceberg climatology the iceberg deterioration rate is also an important factor.

The main currents systems and thus the ice drift are not known in detail for the Barents Sea leaving some uncertainty for the large scale drift of the icebergs. Nevertheless some features are known and the main current systems for Barents Sea are visualized in Fig. 1.1. For icebergs the cold currents moving southwestward from Franz Josef Land and the southeastward current from the eastern Svalbard are the most important current systems for bringing icebergs to the Barents Sea. The Barents Sea is a shallow area with a maximum depth of about 500 m. Due to the rotation of the earth (or more exact due to conservation of potential vorticity), ocean currents tend to flow along depth contours for the case of weak stratification (LaCasce, 2000; Nøst & Isachsen, 2003; Walin, 1972). The validation of the current model also showed that the currents to a large degree follow depth contours (Broström et al., 2009). Accordingly, we expect that topography will play an important role in the Barents Sea, and we expect that icebergs will tend to follow depth contours.

¹ In fact, it takes only a relatively minor ice thickness and ice concentration for the ice to trap the iceberg, which thus starts to move with the ice (Lichey and Hellmer, 2001, Savage, 2008).

For 1987-1992 (the years of the IDAP study, see section on the IDAP study below) it seems reasonable to assume that most icebergs originated from Franz Josef Land (Spring, 1994). However, the large number of icebergs during 1988 was probably from a glacier surge; it is not known which glacier that surged, and the Svalbard glaciers cannot be ruled out. Further discussions on iceberg climatology for the Barents Sea can be found elsewhere (Abramov, 1992; Zubakin et al., 2004; Zubakin et al., 2005).

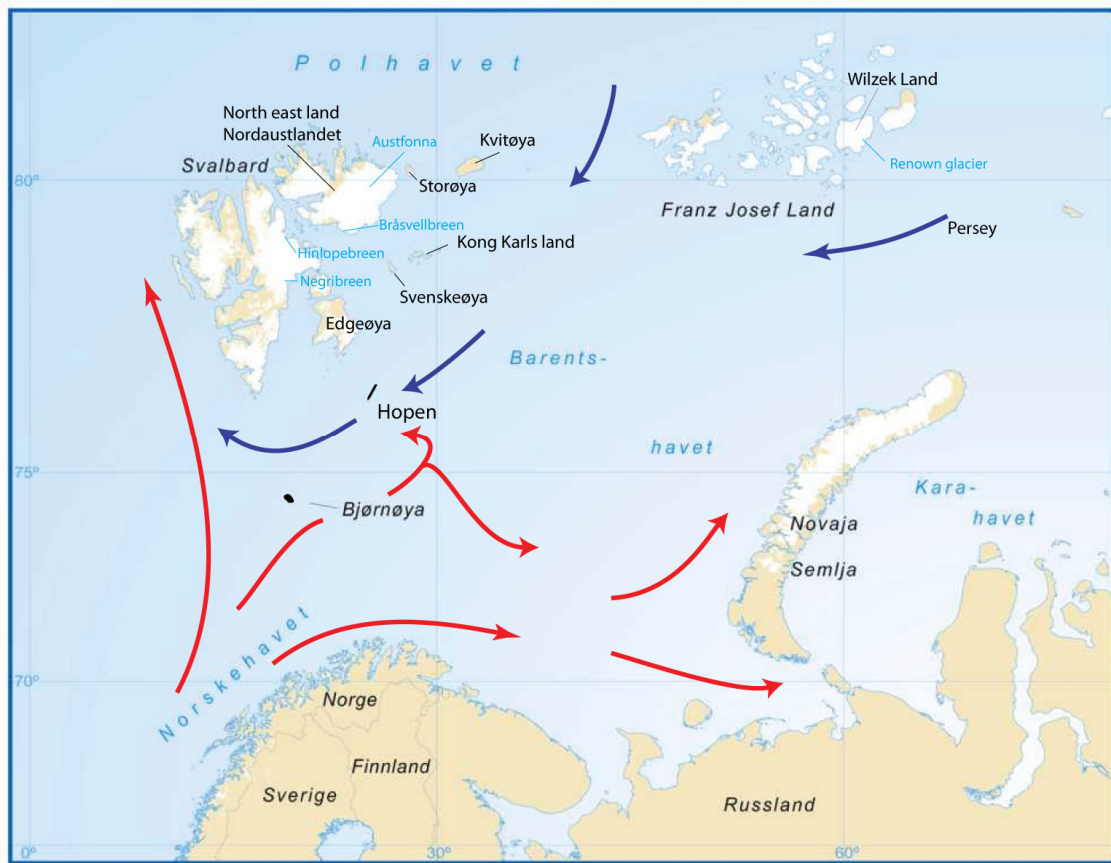


Figure 1.1: Map of the Barents Sea area. Blue text corresponds to glaciers that are important producers of icebergs for the Barents Sea. Red arrow represents warm currents while blue arrow represents cold currents.

1.2 The IDAP study

The most comprehensive studies of icebergs in the Barents Sea was the Ice Data Acquisition Program (IDAP) carried out between 1986 and 1994, where the main investigations were concentrated to 1987-1992 (Løset & Carstens, 1996; Spring, 1994). During the IDAP program some icebergs were tracked using the Argos system. Data on iceberg positions from the Argos system are shown in Figs. 1.2 and 1.3. The figures show that these icebergs take a south-westward path during spring (most data are from spring and summer), consistent with the direction of ocean currents and sea ice movements as discussed above. What is not shown in these figures is that several of the icebergs are grounded at the shallow area north of

Bjørnøya and around Hopen², i.e., the Spitsbergen bank. It is notable that this is a shallow area which is also characterized by strong tides (Gjevik et al., 1994): accordingly, the tidal forcing may provide a mechanism to force the icebergs to get grounded for long times³. The tidal forcing also provides a mechanism to melt icebergs while grounded, due to warm water that flushes by an iceberg that is stuck on the bottom.

It is likely that the origin of the tracked icebergs was Franz Josef Land (Spring, 1994), but it cannot be ruled out that some came from Svalbard. The IDAP study showed that the numbers of icebergs may vary significantly from year to year. The highest numbers of icebergs was recorded in 1988 and was most likely the result of a glacier surge somewhere in the Barents Sea area (Spring, 1994).

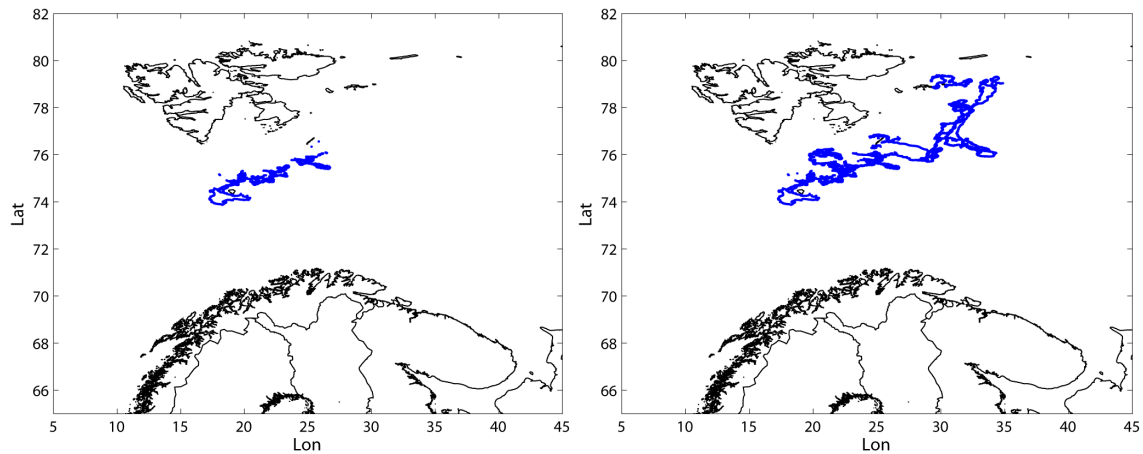


Figure 1.2: Iceberg positions tracked by the Argos system. Left is for 1988 and right is for 1987-1992.

² For instance, several of the icebergs in the IDAP study were grounded for several months. Looking at year 1988 the following icebergs were grounded (at least for the main part of the period): iceberg 3105, March 20 to April 17; 3106 March 21 to June 22; 3109 March 26 to July 15; while icebergs 8893, and 8894 were grounded from March 21 throughout the whole period where data is available (about mid July).

³ Observations show that icebergs can be stuck in this area for months, it is not easy to explain how a melting iceberg can be stuck on the same position for long times. Perhaps the strong tidal forcing can provide large enough velocities to force the iceberg a long way into the shallow grounding zone.

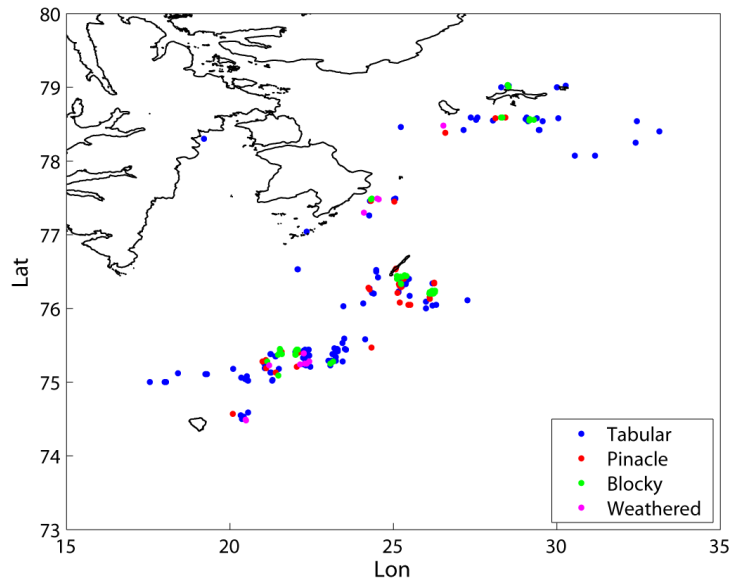


Figure 1.3: All iceberg observations from the 1987-1993 IDAP program. The iceberg sightings appear to be grouped at certain positions and it is not clear why; perhaps some of the observations reflect sightings of the same iceberg?

Before continuing with the model description it is useful to consider some types of icebergs found in the Barents Sea. Frequently observed types are (Spring, 1994)

- Tabular (T): A horizontal or flat-top iceberg with length:height ratio of 5:1.
- Tilted tabular (TT): As a tabular iceberg but the top is tilted.
- Weathered (W): An iceberg which is irregular in shape, due to an advanced stage of ablation; it may have overturned.
- Pinnacle (P): Large central spire or pyramid with one or more spires dominating the overall shape.
- RP: The definition of this class is unknown at the moment but it is likely that it is some type of pinnacle iceberg.
- Blocky (B): Steep precipitous sides with horizontal flat top. Very solid iceberg with length:height ratio of 2.5:1.
- Bergy Bit (BB): Masses of glacial ice calved from an iceberg. Length is within the range 5 -15 m. Height within the range 1 - 5 m.
- Growlers (GR): Masses of glacial ice calved from an iceberg. Length is less than 5 m. Height is less than 1 m.

The definitions follow the WMO Sea Ice nomenclature, except for the tilted tabular which is an added category. The distribution of the iceberg classes are shown in Fig. 1.4. The largest class is the tabular (T and TT) class, and about $\frac{1}{4}$ th of the tabular icebergs are tilted tabular (TT). It does not seem unreasonable that the tilted tabular icebergs are tabular icebergs that have been grounded for some time and become tilted during the time on ground (i.e., due to

inhomogeneous melting due to strong tidal currents)⁴. The second largest class is blocky icebergs (B and BB), while pinnacle icebergs (P and RP) represent say 10% of the sightings. Weathered icebergs (W) are relatively uncommon. The fact that pinnacle icebergs only represent 10% of the sightings has some model consequences as the model was originally designed for pinnacle icebergs. Tabular iceberg geometry has been added to the model as an option and this iceberg class is mainly used in this study; however, this new iceberg model geometry has not been tested against data, and there are some uncertainties regarding the overall shape of the tabular icebergs in the Barents Sea.

An important model parameter is the iceberg geometry. The original model is based on a relation between the iceberg cross-sections area at various heights and depths and the length of the iceberg at the water level, taken from observations of pinnacle icebergs at Grand Banks (Barker et al., 2004; Kubat et al., 2005). For tabular icebergs the situation is more uncertain: in the original CHC code it was suggested that tabular icebergs has a sail height of 7 m and a keel depth of 70 m; the tabular icebergs are thus considered to have an almost rectangular shape.

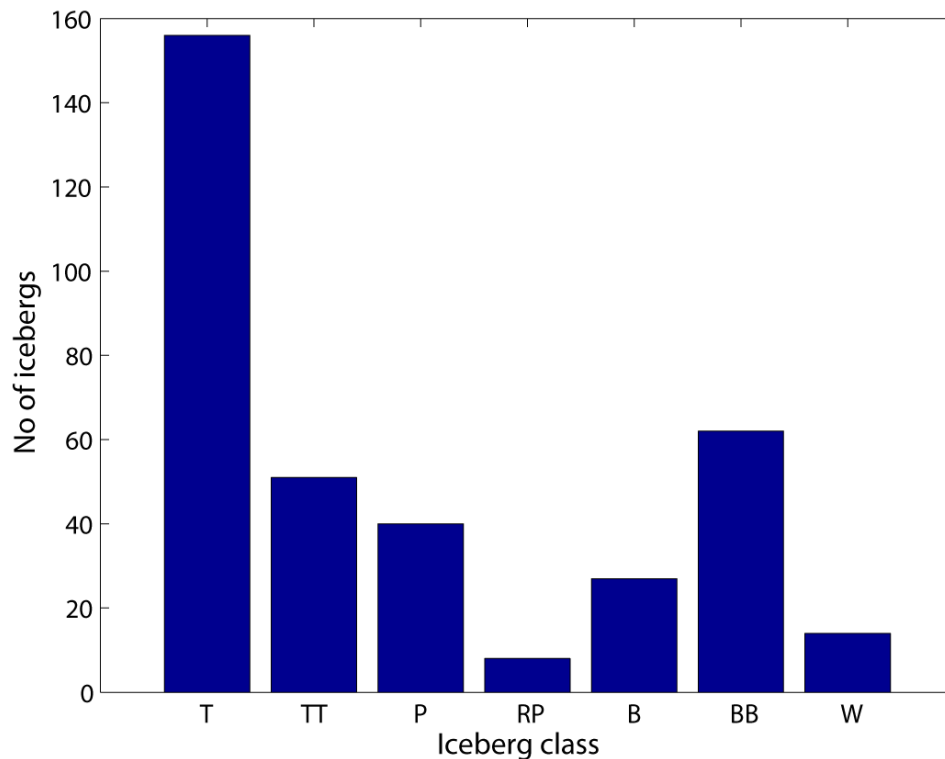


Figure 1.4: The distribution of various iceberg classes in the IDAP database.

⁴ It may also be noted that the tilted tabular class seems to be more typical for Barents Sea than for other areas (the class has to be introduced to describe icebergs in Barents Sea). The combination with stranded icebergs in shallow areas flushed by relatively warm water due to strong tides is also very characteristic for the Barents Sea, which give some indication that the tilted tabular icebergs may arise from these characteristic features of the Barents Sea.

To further investigate the conditions for the Barents Sea we plot the height of the iceberg vs. characteristic iceberg size (i.e. $L_{char} = \sqrt{Length \times Width}$), the result from the IDAP study is shown in Fig. 1.5. First of all we notice that pinnacle, blocky, and weathered icebergs are generally smaller than 100 m, while tabular icebergs may be as large as 300-400 m. For pinnacle, blocky, and weathered icebergs it also seems true that larger icebergs are also higher (and probably deeper) than smaller icebergs. The linear relationship is not very significant but can be spotted by eye in Fig. 1.5. In the CHC model, (pinnacle) icebergs smaller than 50 m are considered to have zero sail area while it is about 1400 m² for a 100 m iceberg. Considering a triangular shape this would correspond to a 28 m high pinnacle iceberg. Perhaps this parameter will need adjustment for Barents Sea given the data shown in Fig. 1.5. Although sail height is not a very important parameter it is a goal of this study to adjust the model to Barents Sea conditions.

For tabular icebergs there is no clear relation between characteristic size of the iceberg and the iceberg height. This is not surprising as there are a large number of source regions for this class of icebergs⁵. However, albeit there is a great scatter, a quick estimate seems to be that the height is 10-15 m, and relatively constant (Fig. 1.5). One relevant question is the thickness of the icebergs and how this relates to size. Unfortunately, we cannot base any discussion on observational proof: nevertheless, it is an important factor and we need to address this question. Observations show that many tabular icebergs in the Barents Sea have a sail height of more than 20-30 m, which would suggest that they have a >200 m keel if we consider the icebergs to be of rectangular shape. This seems to be very deep albeit there are no observations to contradict these numbers⁶. It is known that thick ice ridges has a sail:keel=1:5 ratio. In this study we take an intermediate position and propose a sail:keel=1:7 ratio. Accordingly, we suggest that a sail height of 14 m for tabular icebergs and a keel of say 70-100 m should be used for the Barents Sea. This formulation may need more testing before being included in the model.

One significant observation is that pinnacle, blocky and weathered icebergs start to appear at a size of 100 m. It does not seem unrealistic that these types of icebergs may originate from tabular icebergs that have flipped over. If we assume that tabular icebergs become unstable for a height:length=1 ratio, we find some evidence that tabular iceberg has a total height of 100 m, in some agreement with the discussion above. In the same way, we can explain the fact that there are no small icebergs with large sail heights, most likely because they will turn over when the height:length ratio becomes to large.

⁵ It is likely that the geometry of tabular icebergs is governed by the glacier at the source region since melting does not alter the geometry in any significant way in the initial stage of the deterioration.

⁶ The few available measurements do indicate that large icebergs are deeper than say 70 m albeit there are uncertainties in these estimates (Spring 1994).

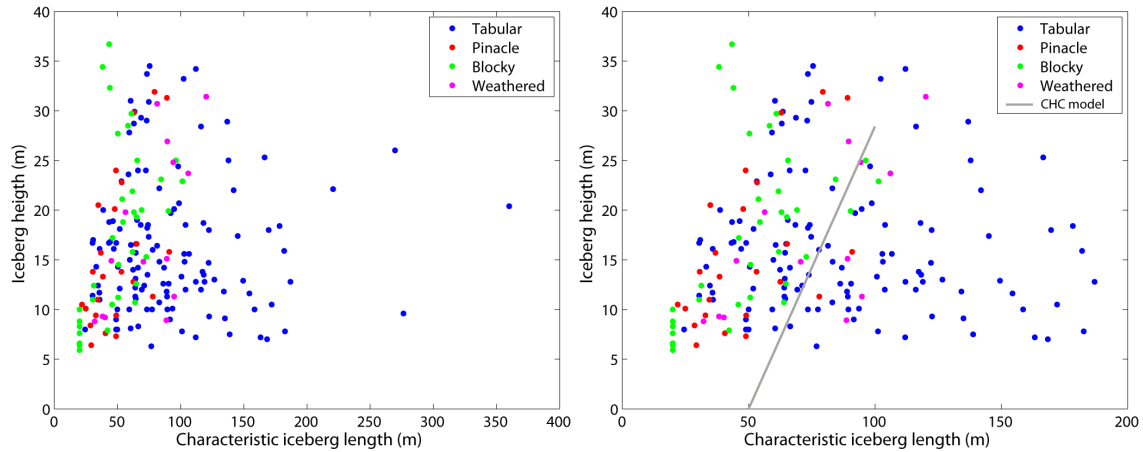


Figure 1.5: Scatter plot of the iceberg height as a function of the characteristic iceberg size (here defined as $\sqrt{Length \times Width}$). For pinnacle and blocky icebergs it appears that large horizontal size implies a high iceberg. For tabular icebergs this relations is not so clear. On right panel (which is a copy of the figure left panel but where the x-axis is limited to 200 m), the CHC sail height (Barker et al., 2004; Kubat et al., 2005) is shown for the case with a triangular shape of the sail. For tabular (rectangular) icebergs the sail height indicated by the CHC formula would be $\frac{1}{2}$ of the gray line.

1.3 Aim of study

The overall aim of the project is to develop an iceberg model for the Barents Sea that can be used for:

1. Hindcasting movements of icebergs in the Barents Sea.
2. Risk predictions based on model estimates of iceberg probability distribution and size in the Barents Sea area.
3. Enabling a forecast system for icebergs in the Barents Sea.

To achieve these goals it is important to validate the model system to ensure that it gives reasonable results. The present study focuses on the iceberg drift and deterioration model, the validation of the hindcast model is described elsewhere (Broström et al., 2009)

The remainder of this document contains three parts each presented in a separate section:

1. Outline of the iceberg model.
2. Validation of the iceberg model.
3. Discussion.

2 Iceberg model

The iceberg model code is documented in a separate report (Sayed, 2008). It is of some interest to outline the model as it will be discussed in the following sections. The model is based on conservation of momentum and conservation of mass.

2.1 Momentum balance

The momentum balance of an iceberg is written as

$$m \frac{d\mathbf{u}_B}{dt} = \mathbf{F}_A + \mathbf{F}_W + \mathbf{F}_C + \mathbf{F}_P + \mathbf{F}_{SI}, \quad (1)$$

where $m=(M_{berg}+m_{added})=1.5M_{berg}$ is the mass of the iceberg and the (added) mass of water that the iceberg drag along its movements (taken to be the same for all types of icebergs), $\mathbf{u}_B=(u_B, v_B)$ is the iceberg velocity in the $\mathbf{x}=(x, y)$ direction, \mathbf{F}_A is the air drag, \mathbf{F}_W is the water drag, \mathbf{F}_C is the Coriolis force, \mathbf{F}_P is the effective force due to pressure gradients in the upper ocean (e.g., due to the sloping sea surface), and \mathbf{F}_{SI} is the force due the iceberg-sea ice interaction.

The wind drag is formulated as

$$\mathbf{F}_A = \frac{1}{2} \rho_A C_A A_A |\mathbf{U}_A| \mathbf{U}_A, \quad (2)$$

where ρ_A is the density of air, C_A is a non-dimensional drag coefficient, A_A is the cross section area (or sail area), and \mathbf{U}_A is the wind speed; index A indicates that it is for air. For water drag the force on the iceberg is

$$\mathbf{F}_W = \frac{1}{2} \rho_W C_W \sum_k A_W(k) |\mathbf{U}_W(k) - \mathbf{u}_B(k)| \mathbf{U}_W(k) - \mathbf{u}_B(k), \quad (3)$$

where index W relates to water properties, and k is the vertical levels in depth (i.e, the model is based on tabulated functions of A_W given at every 10 m depth). It is likely that the stratification in the upper ocean can also contribute to the water drag (or internal wave drag in this context) due to generation of internal waves (Pite et al., 1995), but this affect is not considered here. One key feature of the CHC iceberg model is that it is developed for pinnacle icebergs (characteristic for Grand Banks area) and uses an empirical relation for the area of an pinnacle iceberg (and the sail height and depth of the iceberg) both above and below the water surface. The sail area, A_A , is given by

$$A_A = a_0 L + b_0, \quad (4)$$

where L is waterline length of the iceberg, and $a_0=28.194$ m, $b_0=-1420.2$ m² are empirical constants (Barker et al., 2004; Kubat et al., 2005). In case the expression gives negative value of sail height (i.e, for L smaller than about 50 m) the sail area is set to zero. The area beneath the water surface, A_W , is in a similar way given by

$$A_W(k) = a_k L + b_k, \quad (5)$$

where a_k, b_k are empirical constants determined at every 10 m interval in the deep (Barker et

al., 2004; Kubat et al., 2005). The Coriolis force is given by

$$\mathbf{F}_c = m\mathbf{f}\mathbf{k} \times \mathbf{u}_B, \quad (6)$$

where f is the Coriolis parameter. The pressure gradient in the water is given by (Savage, 2001)

$$\mathbf{F}_p = m \left(\frac{d\overline{\mathbf{U}}_w}{dt} + \mathbf{f}\mathbf{k} \times \overline{\mathbf{U}}_w \right),$$

where

$$\overline{\mathbf{U}}_w \approx \frac{\sum_k A_w(k)^2 \mathbf{U}_w(k)}{\sum_k A_w(k)^2},$$

is the weighted water current between the sea surface and the keel depth. Note that this formulation is different from more standard formulations based on the pressure gradient from a sloping sea surface (Savage, 2001). In the present model a simpler formulation is used such that

$$\mathbf{F}_p = m\mathbf{f}\mathbf{k} \times \overline{\mathbf{U}}_w, \quad (7)$$

where

$$\overline{\mathbf{U}}_w \approx \frac{\sum_k A_w(k) \mathbf{U}_w(k)}{\sum_k A_w(k)}.$$

The radiation force from waves is described by (Longuet-Higgins, 1977; Savage, 2007)

$$\mathbf{F}_r = \frac{1}{2} \rho_w C_{wd} g L H_w^2 \mathbf{k}_w, \quad (8)$$

where $C_{wd}=0.3$ is the wave force coefficient, g is gravity, and H_w is the wave height⁷, finally \mathbf{k}_w is the direction of the waves. For wind waves the radiation stress is taken to be in the wind direction, i.e., $\mathbf{k}_w = \mathbf{U}_A / |\mathbf{U}_A|$, while for swell the wave radiation stress is in the direction of the swell (the swell direction is thus taken from the wave model).

For the ice force on an iceberg Lichey and Helmer (2001) gave following expression

$$\mathbf{F}_{SI} = \begin{cases} 0, & A_{SI} \leq 15\%, \\ \frac{1}{2} \rho_{SI} C_{SI} A_{SI} |\mathbf{u}_{SI} - \mathbf{u}_B| (\mathbf{u}_{SI} - \mathbf{u}_B), & 15\% \leq A_{SI} \leq 90\%, \\ \infty |\mathbf{u}_{SI} - \mathbf{u}_B| (\mathbf{u}_{SI} - \mathbf{u}_B), & 90\% \leq A_{SI} \text{ and } P \geq P_{SI}, \end{cases} \quad (9)$$

⁷ Wave height is twice the wave amplitude; the wave model gives significant wave height (H_s), which is related to the wave height as $a_w = H_s / 1.421573$ (Savage, 2007). Note that this expression is very similar to $a = H_s / \sqrt{2}$, as would be given by standard derivation of significant wave height and wave height (Komen et al. 1994; Phillips, 1977)

where \mathbf{u}_{SI} is the sea ice velocity, A_{SI} is the sea ice coverage, P is the stress on the iceberg from the ice and P_{SI} reflects the value for which the ice resist the forces acting on the iceberg without failing (Lichey & Hellmer, 2001; Savage, 2008). The constant C_{SI} depend on the ice strength, or the effective ice failure pressure, and the CHC model is based on the description of C_{SI} given by Savage (2008). The formulation in Eq. (9) for high ice concentration ($A_{SI} \geq 90\%$) essentially implies that the iceberg is frozen in the ice and will move with the ice speed⁸. As a note, it is considered as common knowledge that the ice will move with 2-8% of the wind speed, and having a reflection of 15-20° to the right of the wind direction due to the rotation of the earth. In severe ice conditions we therefore expect the icebergs to move relatively fast in strong wind conditions. We emphasize that the sea ice force on icebergs is not included in the original CHC model used at Grand Banks and will need validation. The CHC model is somewhat different than the original Lichey and Helmer model, and by request from StatoilHydro the original Lichey and Helmer model has also been included as an option in the present code.

To numerically solve the equations an implicit Euler scheme is used since an explicit Euler scheme is unstable when the Coriolis force is included. To apply the implicit formulation, a Taylor expansion is used to find a linear function of the velocity \mathbf{u}_B at time $t+\Delta t$ (Kubat et al., 2005; Savage, 2001). The standard time step is taken to be 2 min (Sayed, pers, comm.); the model is started with zero initial velocity of the icebergs, this will not affect the forecast significantly on timescales longer than 1 hour.

2.2 Deterioration module (or mass balance)

The deterioration of icebergs is more complex to describe than its motion. The deterioration will depend on the geometry of the iceberg and how it interacts with the surrounding elements. This interaction is very complex to describe and the present formulation is based on empirical relations found over many years. The most important processes, and their relative magnitudes, are listed below (Savage, 2001)

1. Wave induced erosion (say 60 %).
2. Wave induced calving (say 20%).
3. Forced convection in water (say 15%).
4. Solar radiation (say 3.5%).
5. Buoyant convection in water, wind convection (say 1.5%).

For large icebergs, cracking of icebergs by wave bending may also be important (Squire, 2007; Squire et al., 1995; Wadhams, 2000); this is not included in this study. The readers are also referred to other studies for a more detailed description of the deterioration processes (Kubat et al., 2007; Savage, 2001). We note that many of the following expressions for melt rates are based on empirical formulas. Those formulas involve coefficients evaluated to give the melt rates in units of m/s. The units of those coefficients are not listed here, as customary done in similar literature (e.g. White et al. 1980, and Savage 2001).

⁸ This is also the way that "frozen in" icebergs are treated numerically in the model. The icebergs are advected with the speed of the sea ice.

2.2.1 Model description

One important factor in the model is the relation between iceberg mass and waterline length. Here we use

$$M = \kappa \rho_i L^3, \quad (10)$$

where ρ_i is ice density. The parameter κ has a value of approximately 0.45 (Barker et al., 2004): based on iceberg observations both from AARI and IDAP studies, this seem to be somewhat high and value around 0.35 may be more appropriate for Barents Sea (K. Johannessen, Personal communication). The deterioration will here be expressed as a velocity representing the rate of change of the waterline length of the iceberg, the total loss of mass needs to be calculated using Eq. (10).

Surface melting due to solar radiation

The melting velocity for solar radiation I is given by (Savage, 2001)

$$V_s = \frac{I}{\Gamma \rho_i} (1 - \alpha), \quad (11)$$

where Γ is the latent heat of melting of ice (334 kJ/kg), and α is the albedo. The values of the albedo range from 0.1 for clear ice surfaces to 0.95 for fresh snow: $\alpha=0.7$ is used in the present model. The solar insolation for Barents Sea varies significantly; however, here we use a constant value of 203.5 Wm^{-2} . The model is not very sensitive to the exact value of this parameter.

Melting due to buoyant vertical convection

An iceberg will affect the density of the water in the vicinity of the iceberg. Accordingly, density driven currents will be induced that affect the melting of the iceberg. The dynamical feature of this process is very complicated and the following empirical correlation is used to estimate the melt rate (Neshyba & Josberg, 1980)

$$V_b = 2.78(\Delta T) + 0.47(\Delta T)^2, \quad (12)$$

where ΔT is the difference between the far field water temperature, T_∞ , and the freezing point temperature, T_{fp} ; i.e. $\Delta T = T_\infty - T_{fp}$. Note that to convert V_b to units of m/s, Eq. (12) should be divided by 31,536,000 (Kubat et al., 2007).

The equation for the freezing point to be used in the model is

$$T_{fp} = T_f(S) e^{-0.19(T_\infty - T_f(S))}, \quad (13)$$

where T_∞ is the far field water temperature (away from the immediate surface of the iceberg), and T_f is the sea water freezing temperature based on the far field salinity, S . The sea water freezing temperature depends on the salinity, S , according to (Løset, 1993)

$$T_f(S) = -0.036 - 0.0499S - 0.000112S^2. \quad (14)$$

The range of salinity values is $1.77\% \leq S \leq 3.5\%$. However, in the code, the value of T_f is -1.86°C .

Forced convection

The relative velocity between the iceberg and water current contribute to the process of melting the keel (the relative velocity between the iceberg and the water is important to replace the cold water close to the iceberg with warm sea water). Also wind can contribute to melting of the sail and this is described in a similar way as the melting in water. The surface melt due to forced convection can be expressed as

$$V_f = \frac{q_f}{\rho_i \Gamma}, \quad (15)$$

where q_f is the heat flux,

$$q_f = Nu k_f \Delta T / L, \quad (16)$$

where k_f is the thermal diffusivity of the fluid (air or sea water). The Nusset number, Nu is given by

$$Nu = C Re^{0.8} Pr^{0.4}, \quad (17)$$

where $C=0.058$, and the Reynolds number, Re , and Prandl number, Pr , are defined as

$$Re = V_r L / \nu, \quad (18)$$

and

$$Pr = \nu / k_f. \quad (19)$$

Here V_r is the relative velocity between the iceberg and the fluid and ν is the kinematic viscosity. We note that in calculations of the drag forces, which are used in modelling the drift, the variation of water current with depth is taken into account (Kubat et al., 2005). However, for the above calculation of the relative velocity, V_r , a mean current was considered to give adequate accuracy and is consistent with overall formulation that is based on observations.

Wave erosion

This is a major source of iceberg deterioration. White et al. (1980) developed the following equation to estimate the melt rate of a notch at the waterline

$$V_{we} = 0.000146 \left(\frac{R}{H} \right)^{0.2} \left(\frac{a_w}{\tau} \right) \Delta T, \quad (20)$$

where V_{we} is the melt rate in m/s, R is the roughness height of the ice surface, typically 0.01 m (White et al., 1980), ΔT is the temperature difference between the sea water and the iceberg (defined below Eq. (12)), and τ and H_w are the wave period and wave height in units of seconds and meters, respectively. The melt rate V_{we} can be up to 1 m/day for a 1 degree C temperature difference. This shows that ΔT must be known with high accuracy to evaluate melting in a reliable way.

Calving

Calving can be caused by several mechanisms but the most important is the breaking of overhanging slabs of ice (Savage, 2001). A notch at the waterline usually forms due to wave

erosion. As the erosion progresses, the notch deepens and size of the ice hanging above the notch increases. At a certain stage, the bending stresses cause fracture of the ice, and the overhanging slab collapses. The model mimicking this process (White et al., 1980) can be summarized as follows: the critical length of an overhanging slab at which fracture (calving) occurs, F_l , is given by

$$F_l = 0.33(37.5 H_w + h^2)^{1/2}, \quad (21)$$

where H_w is the wave height and h is the thickness of the overhanging slab (both in meters). The expression for the overhanging slab thickness can be expressed as (Savage, 1999)

$$h = 0.196 L. \quad (22)$$

For steady wave action, the calving interval, t_c , is given by

$$t_c = F_l / V_{we}. \quad (23)$$

Savage (1999) also carried out an analysis of the shape of the overhanging ice and obtained the following expression for the calved ice volume,

$$\bar{V}_c = 0.64 L F_l h. \quad (24)$$

The above correlations were verified using available estimates of observed calved ice masses (Savage 2001). Aside from the mechanism discussed here, calving can occur due to fracture caused by internal stresses or overturning. Such mechanisms appear to have a minor contribution to calving (Savage, 2001). They are also too complex to include in the present simple mechanical model.

3 Validation of the iceberg model

This section describes the verification and the validation of the iceberg model implemented at met.no. To verify the model, the code formulation has been discussed on many occasions and there have been two one-week exchanges of personnel between met.no and CHC. The model has been verified during these discussions, and the model results show similar results for trajectories as the oil drift model (OD3D) used at met.no (not shown). Furthermore, the grounding capability of the model has been tested and appears to work. Switching the iceberg forces on and off is demonstrated. The model has been run with up to 100.000 icebergs (with random seeding of the initial position of the icebergs applying a Gaussian bell distribution) and all icebergs travel in a similar way (although we do expect some dispersion of the icebergs (LaCasce, 2008)).

The following sections describe the iceberg behavior in both observations and model, and outline differences between modeled iceberg trajectories and observed trajectories. It should be noted that this constitutes a rather large and diverse dataset and a detailed comparison between the iceberg hindcast and the observed trajectories is a complicated task. One of the largest unknowns for the iceberg model is that we do not know the geometrical shapes of the icebergs. We have removed the grounding of icebergs in this study as we did remove all observations with grounded icebergs. There are large uncertainties in the bottom topography on the fine scale and the actual size of the icebergs such that the grounding in the model/observations is very uncertain at the moment. Finally it should be pointed out that the largest source of error is probably inaccuracies in the hindcast of ocean currents, and possibly also ocean temperature for the case of iceberg deterioration (Broström et al., 2009).

3.1 Forcing data

To force the iceberg model we need data on

1. Atmospheric wind (in principle we also need air temperature and solar radiation; however in the present model air temperature is approximated with the sea surface temperature, and a fixed solar radiation is accurate enough for the present purpose).
2. Ocean currents and temperature.
3. Significant wind-wave height, significant swell-wave height and swell direction.

For the present study we aim at a hindcast for the period August 1987-August 1988, and the data we use to force the model are described below. It should be noted that the hindcast data are not fully consistent with each other as the atmospheric fields were not used to force the ocean/ice model.

- The atmospheric hindcast run was based on the ERA40 model data and was downscaled at met.no using the HIRLAM-5 model (Undén et al., 2002).
- To create hydrography and currents for the year of 1988 we used a coupled numerical ocean-ice model, i.e., the MIPOM MI-IM code (Engedahl, 1995; Røed & Debernard, 2004). The coupled ocean-ice model covers the Barents Sea region and part of the Nordic Seas, with a 4km horizontal resolution. The atmospheric forcing fields were taken from the ECMWF ERA-40 reanalysis (<http://www.ecmwf.int/research/era/do/get/era-40>). Tidal forcing included eight

harmonic constituents (M2, S2, N2, K2, Q1, O1, P1 and K1) gathered from barotropic tidal models (Flather, 1981; Gjevik, 1990). In addition, sea surface temperature (from ERA-40) and merged ice concentration fields (a combination of data from the ice service of the Norwegian Meteorological Institute and the ERA40 data-set) were assimilated via a nudging scheme (Albretsen & Burud, 2006).

- The wave model is based on the WAM model (Cavaleri, 2007; Komen et al., 1994), which predicts the wave energy in different directions for various frequency intervals. The wave model is forced with the met.no reanalysis described above.

3.2 iceberg drift

Let us start with a figure showing the data for 1988. We have removed all data points where the icebergs seem to be grounded or when there is a large temporal gap in the data. Iceberg 3105 has the best data coverage and we will exemplify much of the basic discussion based on Iceberg 3105.

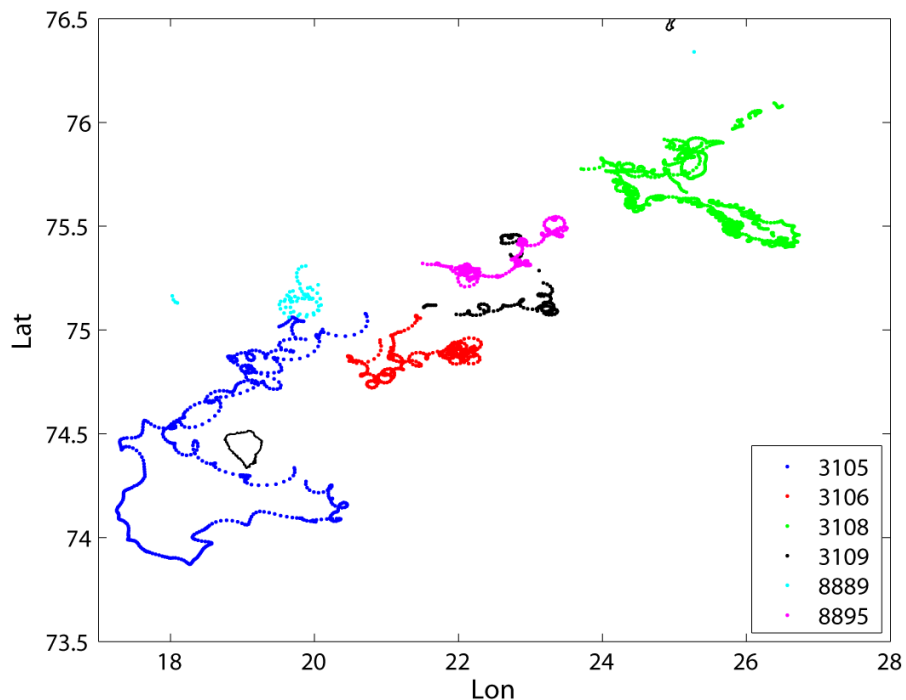


Figure 3.1: A plot of all IDAP data for 1988. The numbering of the icebergs refers to their number in the Argos tracking system. Bjørnøya is located in the lower left and the Hopen Island is at the top near 25° E.

3.2.1 Experiments with different iceberg type and iceberg size

Below we describe maps showing modelled iceberg trajectories released at observed positions taken from the IDAP database together with real movements of the icebergs. We use a three day hindcast and each plot contains three experiments released at midnight one day apart (i.e., the model icebergs were released 24 h apart at 0h, 24h, 48h). Observational data for six days are shown in each figure. We have chosen to use the first 18 days of data from iceberg 3105

(starting at midnight April 18), and the iceberg moves in vicinity of Bjørnøya during this time.

In the next few pages (i.e., Fig. 3.2-3.5), experiments with the following iceberg geometries are visualized:

- Tabular 100 m.
- Tabular 100 m, and tabular 150 m.
- Tabular 100 m, and pinnacle 100 m.
- Pinnacle 50 m, pinnacle 75 m, and pinnacle 100 m.

Overall we find that (Fig. 3.2-3.5)

- The main direction of the drift hindcast is satisfactory.
- Iceberg velocity is good (judging from the distance between the points representing data 1 h apart), this will be further investigated in Section 3.3.
- Shape of the movements is good (i.e., the icebergs often take an elliptic trajectory due to tidal and inertial movements). This is an important factor when we want to analyze the risk of a certain position being hit by an iceberg (Korsnes & Moe, 1994; Zubakin et al., 2005).
- The modeled trajectory is not very sensitive to iceberg size for large icebergs. It is noted that iceberg size is likely to be most important for small pinnacle icebergs. Tabular icebergs do not change their geometry while deteriorating, while the shape of pinnacle icebergs changes when they deteriorate.

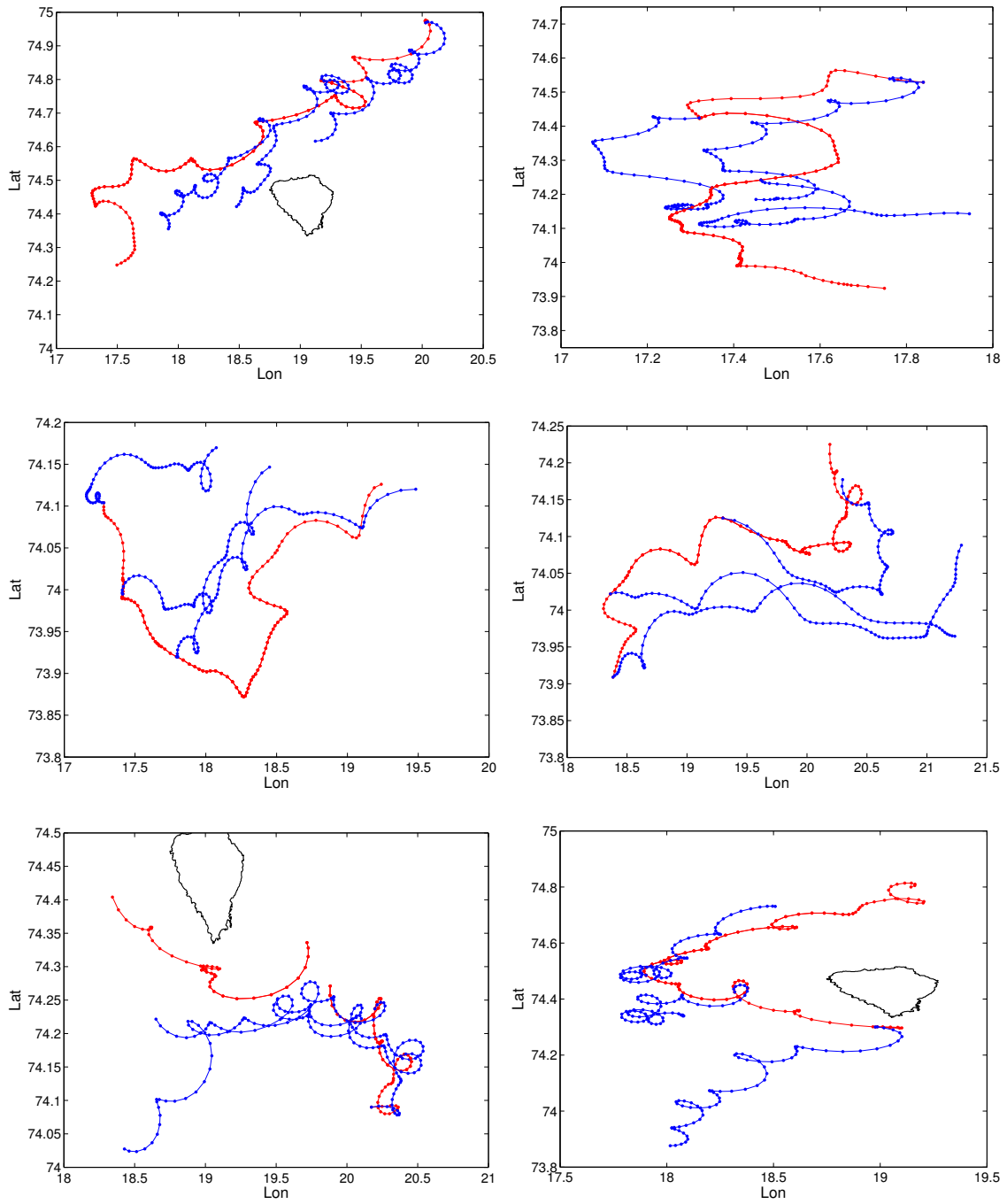


Figure 3.2: Observed and modeled trajectories of iceberg 3105. Red is 6 days of observed data and blue is three model runs started at midnight. Each model run continues for 3 days. Blue is for a tabular iceberg size 100 m.

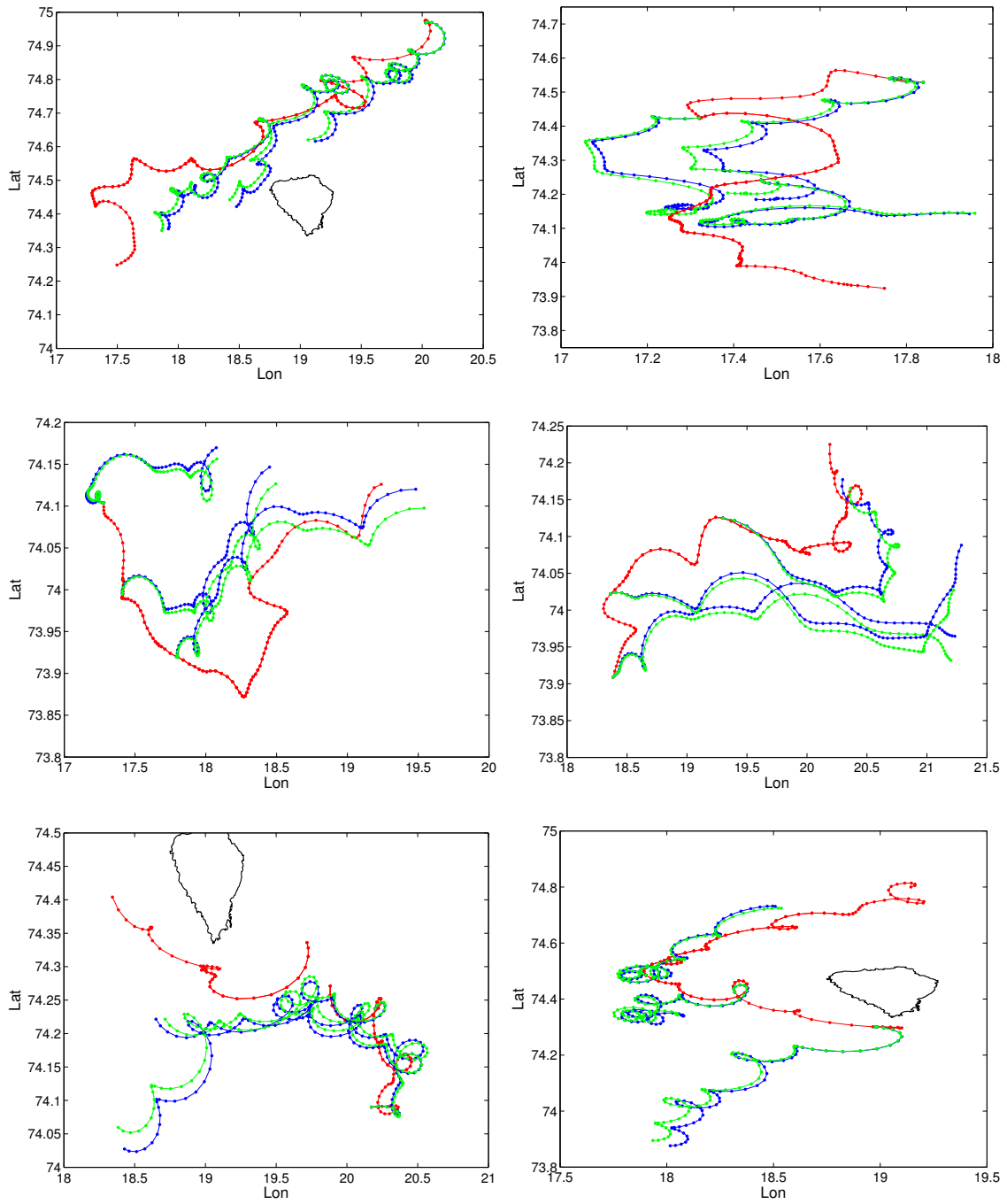


Figure 3.3: Observed and modeled trajectories of iceberg 3105. Red is 6 days of observed data and blue is three model runs started at midnight. The model runs continue for 3 days. Blue is for tabular iceberg size 100 m, and green is for tabular iceberg with size 150 m.

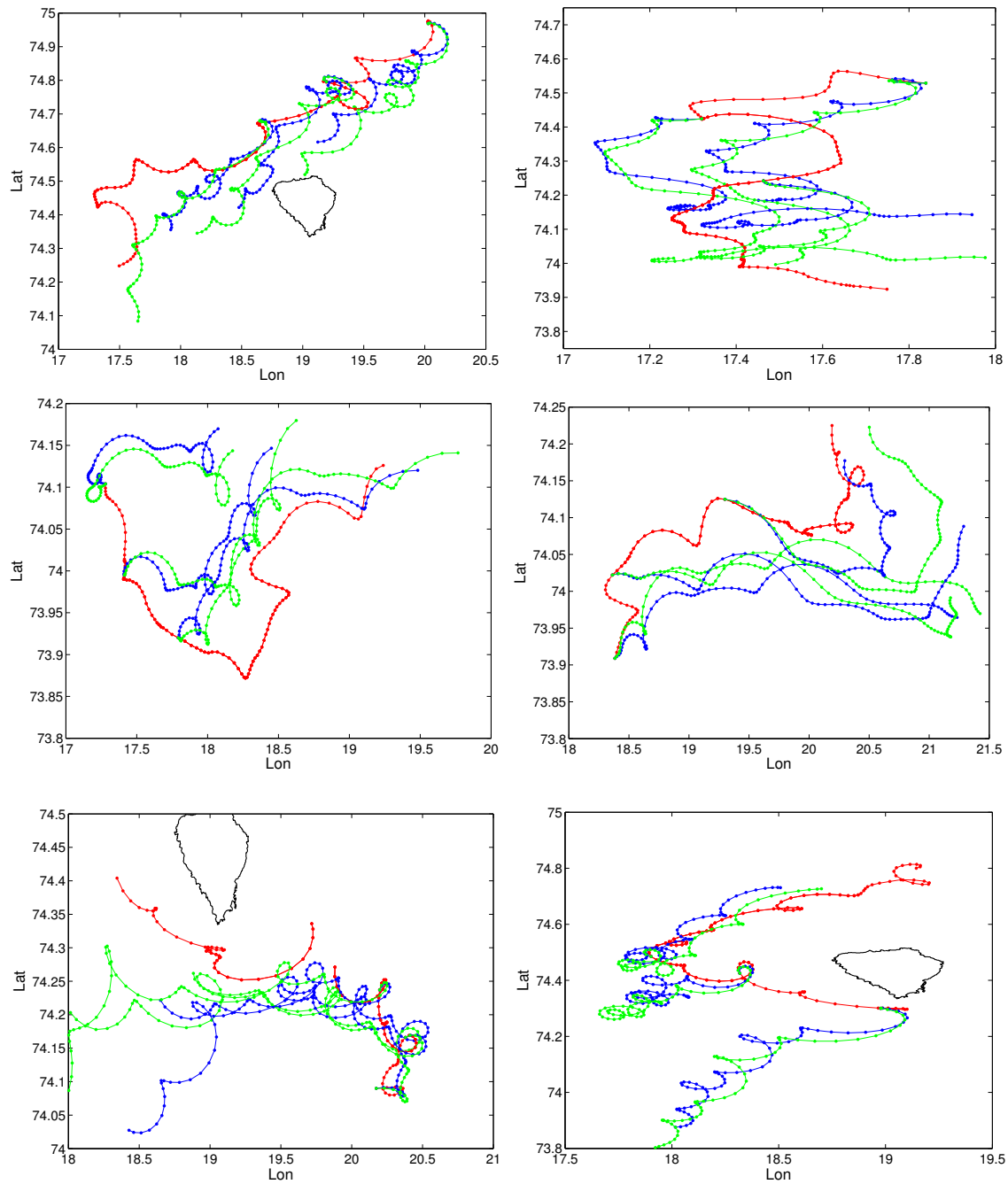


Figure 3.4: Observed and modeled trajectories of iceberg 3105. Red is 6 days of observed data and blue is three model runs started at midnight. The model runs continue for 3 days. Blue is for a tabular iceberg size of 100 m and green is for a pinnacle iceberg size of 100 m.

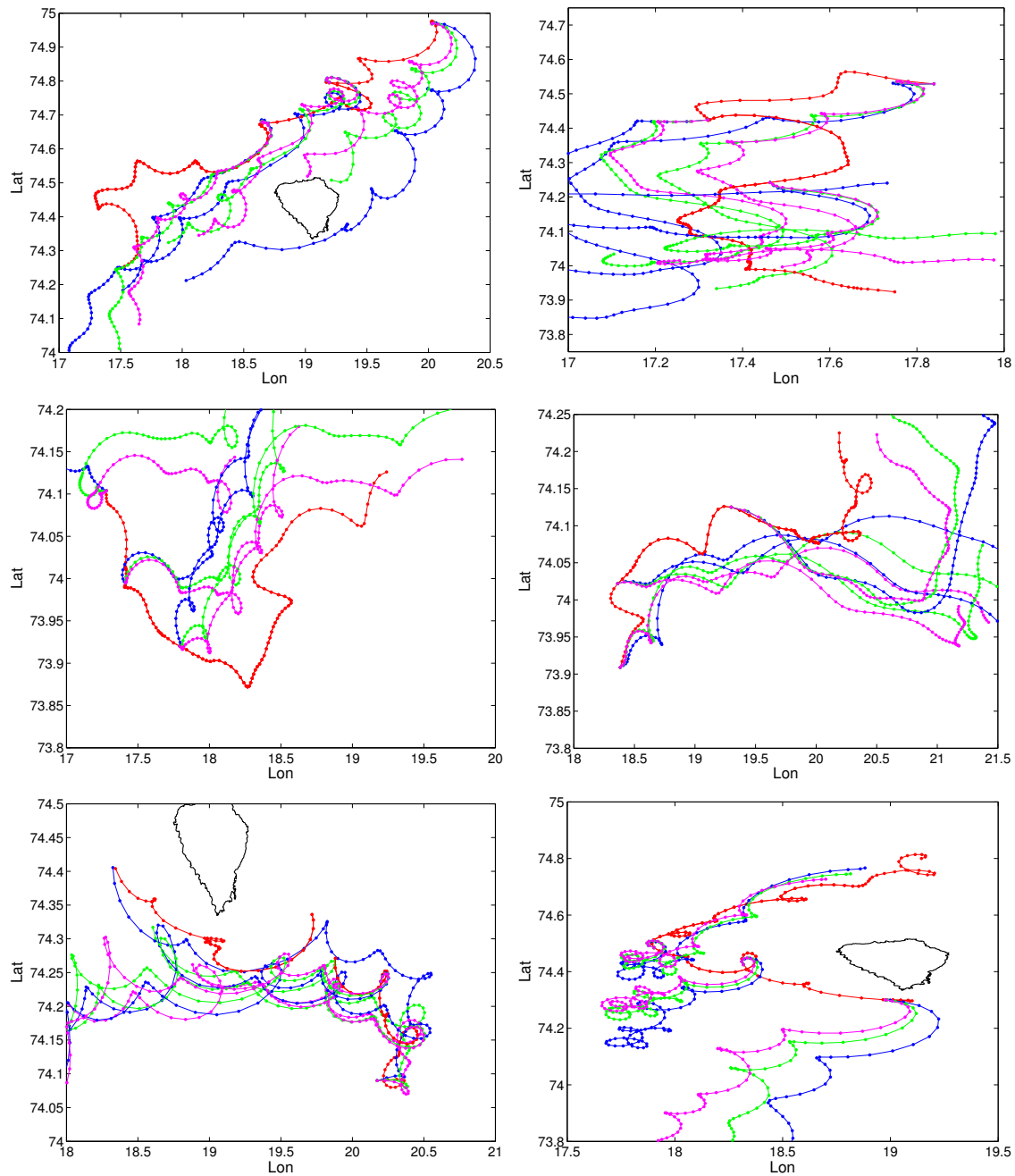


Figure 3.5: Observed and modeled trajectories of iceberg 3105. Red is 6 days of observed data and blue is three model runs started at midnight. Each model run continues for 3 days. Blue, green, and cyan are for pinnacle icebergs with sizes 50 m, 75 m and 100 m, respectively.

3.2.2 Experiments with various forcing

The drift of the icebergs depends on the strength of the different forcing mechanisms, and StatoilHydro has expressed a wish to be able to turn off the different forces described in Sec. 2. To verify the model setup and to study the sensitivity of the drift to various forcing factors

we have done some experiments where a certain force has been canceled. The results are shown in Fig. 3.6.

The first observation we make is that the iceberg move very rapidly if the ocean forcing (Eq. 3) is turned off (Fig. 3.6 left panel). The reason is that ocean currents do not only provide a mechanism to force movements of the iceberg, but it does also provide a drag when other forces accelerate the iceberg. Accordingly, when removing this force, the iceberg will accelerate quickly as there are not any forces to decelerate the iceberg. We have therefore chosen to set ocean currents to zero for this option (Fig. 3.6 right panel). For this specific case it is clear that wave forcing is the dominant forcing factor, followed by ocean currents. The wind has a relative strong impact suggesting that we have a situation with high wind speeds (and thus also a strong wave field). The period starts with low wind and weak ocean currents: the wind strength increases with time and is about 8 ms^{-1} after 6 hours and after that it weakens to a few ms^{-1} , the significant wave height is small (order 1.5 m) during this period. The wind increases in strength after 24h from the start of the simulation and reaches a maximum wind speed of, say, 14 ms^{-1} one day later (from the west); now the significant wave height is 3.5 m for wind waves and 1.5 m for swell waves, which does provides a strong force on the iceberg.

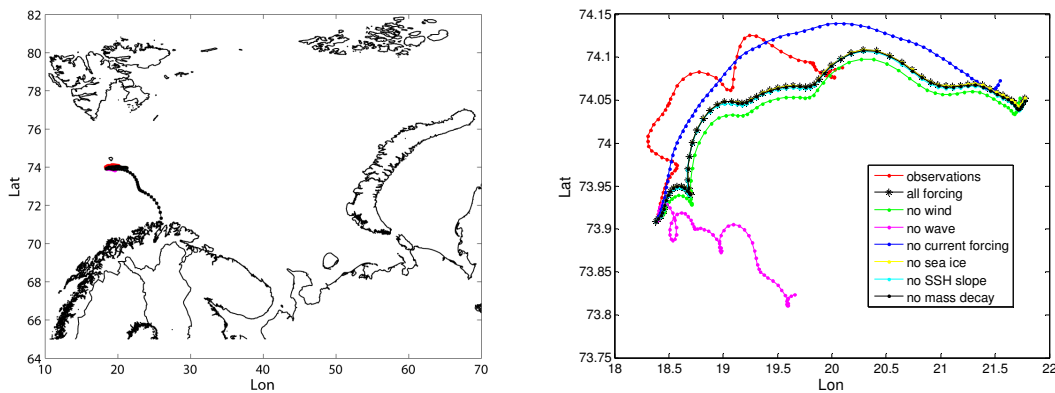


Figure 3.6: The drift of a 100 m tabular iceberg for different setup of the model forcing. Left panel is for turning off the ocean forcing and right panel is for the case with turning of ocean currents for no current forcing.. The result with no current forcing is a very fast acceleration of the iceberg as no limiting forces are present, and we choose the alternative to set the ocean currents to zero instead.

For pinnacle icebergs the mass (i.e., height and keel depth) is an important factor for the iceberg drift. However, for tabular icebergs, as seen from Fig. 3.7, the drift trajectories were not very sensitive to the iceberg size. Accordingly, for short term calculations the iceberg deterioration can be neglected for large tabular icebergs with respect to the drift pattern. For longer trajectories the deterioration is of course important but this case is not considered in the present report. The results for pinnacle icebergs of initial size of 100 m are shown in the right panel in Fig. 3.7. The difference in trajectory paths from model and observations is larger but the difference is not overwhelming. We may conclude that deterioration is most important for small pinnacle icebergs, which deteriorate quickly and thereby change the geometrical features of the iceberg. For large tabular icebergs the influence of melting is small on the hindcasted trajectory path.

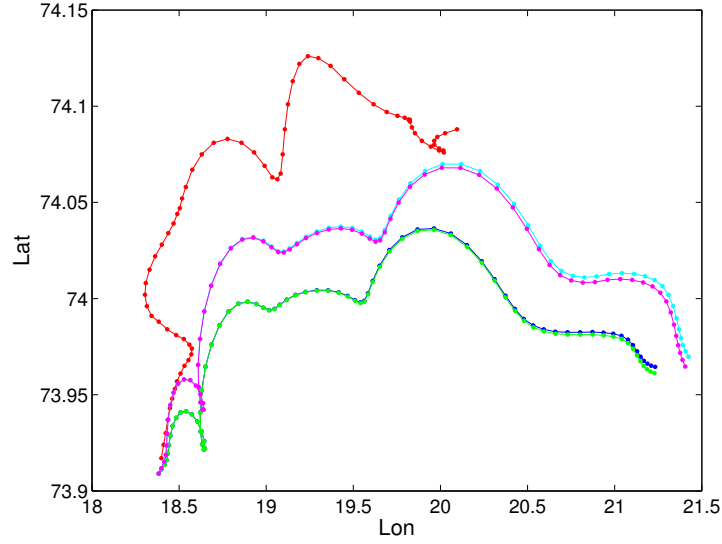


Figure 3.7: The drift of a 100 m tabular iceberg and a 100 m pinnacle iceberg with and without deterioration. Red is observations and upper curves (cyan and magenta) are for pinnacle icebergs and lower curves (blue and green) are for the tabular iceberg.

3.3 Deviation between model and observations

Let us define the distance between the modeled iceberg and the observation as

$$\Delta L(t) = \sqrt{(x_m(t) - x_{obs}(t))^2 \cos^2(y_{obs}(t)) + (y_m(t) - y_{obs}(t))^2} G, \quad (25)$$

where t is the time after the release of the iceberg, (x_m, y_m) , (x_{obs}, y_{obs}) , are the modelled and observed longitude and latitude positions of the icebergs, respectively. $G=4 \cdot 10^4/2\pi$ km/degree is a geometrical factor for converting results in spherical coordinates to km. For some cases it is convenient to see a simple measure of the model performance for the entire set of experiments (e.g., the release of many icebergs at close by positions or different experiments). Accordingly we define an ensemble mean deviation $\overline{\Delta L}$ as

$$\overline{\Delta L}(t) = \frac{1}{N(t)} \sum_{i=1, N(t)} \Delta L_i(t), \quad (26)$$

where $N(t)$ is the total number of model positions and observations at time t (after the release of the icebergs). Notably, $i=1, N$ may reflect a selected part of the experiments and observations (for instance the 18 experiments visualized in Sec. 4.2), or for all 129 experiments that are available. Also note that $N(t)$ must take into account case where data is missing.

Let us starting with visualizing ΔL for the experiments shown in Figs. 3.2-3.5, the results are shown in Fig. 3.8. We see that there is a great scatter of ΔL between different experiments and that the deviation between modeled positions and observations may actually decrease with time under certain circumstances. However, when we look at the mean of all experiments we see that the model error grows with time. After 72 h we have a mean model-observation deviation of about 35 km in these experiments. Another important remark is that there are a

few cases with very large model-observation deviations. Accordingly, we do expect that more than 50% of the experiments will be better than the mean model-mean deviation as defined in Eq. (26).

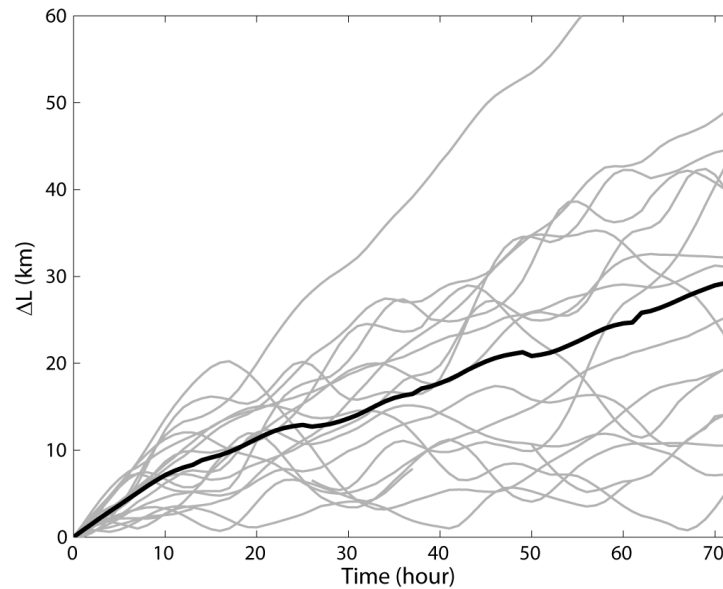


Figure 3.8. Plots of the deviation between modeled and observed positions for a three day hindcast. Data are taken from the first 18 days for iceberg 3105 were the forecast starts at midnights at observed positions. Thin gray lines represent all data in Figures 3.2-3.5 while the thick line is the mean deviation in the experiments.

The model-observation deviations for two different initial tabular iceberg sizes are shown on the left panel of Fig. 3.9. The corresponding deviations for three pinnacle icebergs with different initial sizes are displayed in the right panel. For tabular icebergs there is little difference between the two experiments, while there is a large difference for pinnacle icebergs of different initial sizes. Again we conclude that the main reason is that the geometrical shape of tubular icebergs does not change with size while the cross-sectional area for pinnacle icebergs depends on the iceberg size (Eq. 4 and 5). In these experiments we see that the large pinnacle icebergs represent data more accurate than small icebergs. However, the uncertainties regarding the actual shape of the iceberg imply that it is difficult to make any clear judgment on iceberg size or iceberg shape from these data.

Experiments with different strength of the wave radiation forcing (Eq. 8) are shown in Fig. 3.10. Somewhat surprisingly we find that experiments with both stronger and weaker radiation stress perform somewhat better when compared with data. However, the difference is rather small and at this stage it is fairer to say that all three experiments perform equally well.

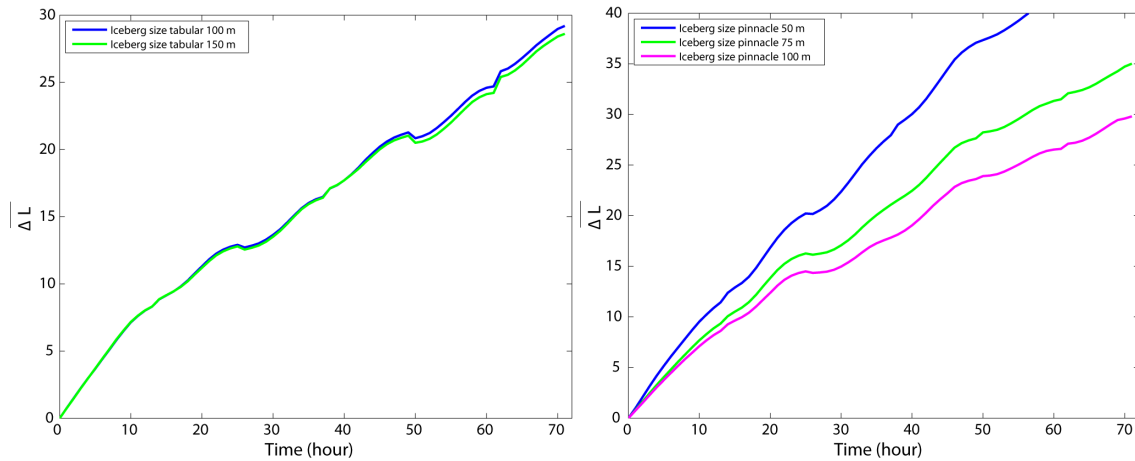


Figure 3.9: Plots of the “ensemble” deviation between modeled and observed positions for the first 18 days, for iceberg 3105. Left panel shows the mean deviation for tabular icebergs with size 100 m (blue) and 150 m (green). Right panels show the cases with pinnacle icebergs with sizes 50 m, 75 m, and 100 m.

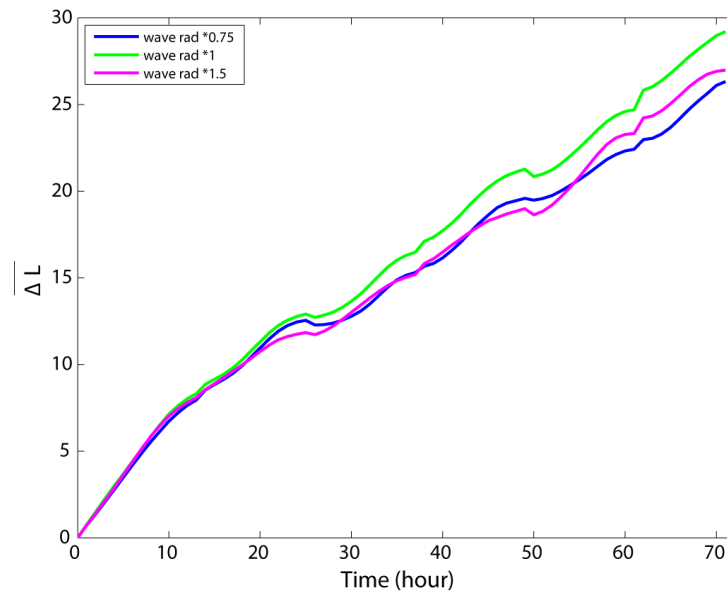


Figure 3.10: Plots of the “ensemble” deviation between modeled and observed positions for the first 18 days, for iceberg 3105. The figure shows different deviations for various wave radiation stresses.

3.4 Model results using all data

In the previous two sections we chose to focus on iceberg 3105, and the first 18 days of the observations. The reason for this selection is to establish a data set that is easy to visualize. However, for a more complete assessment of the model performance we need to address all available data. In Fig. 3.11 the model-observation deviation data from all experiments are plotted. Here we see that most model experiments perform better than the mean deviation as defined by Eq. (26), due to the presence of a few experiments with large model-observation deviations. The mean model-observation deviations for a few model setups are displayed in

Fig. 3.12. In these experiments tabular icebergs with different geometries i.e., high geometry (14 m high icebergs) and high and deep (14 m high, 100 m deep icebergs), are used. We see that changing the size of the tabular icebergs does not change the model performance in any significant way (as was also seen in Figs. 3.3, 3.7, and 3.9). The high tabular iceberg performs somewhat worse while the high and deep iceberg performs somewhat better than the standard experiment. We also see that the experiment with weak wave forcing performs best in the present set of experiments. However, given the large unknowns in the iceberg geometry, it is not possible to make any reliable statement on how to tune the strength of the different forcing variables.

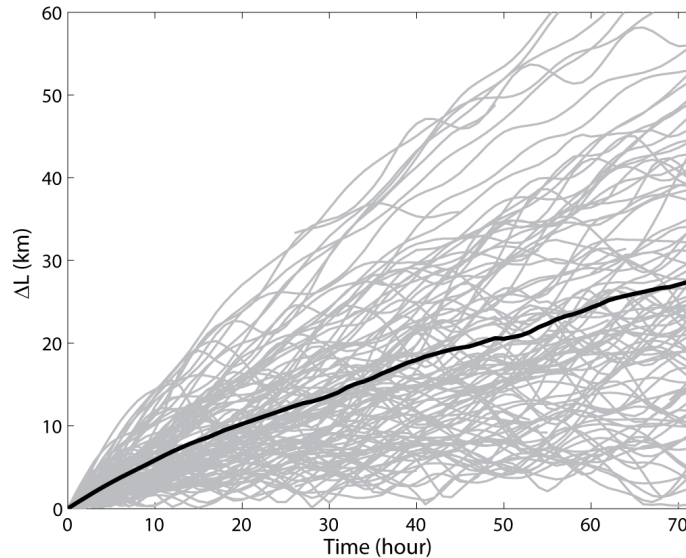


Figure 3.11: The deviation between modeled and observed positions for all available data. Thin gray lines are from each experiment, and thick line is the “ensemble” mean deviation in the experiments.

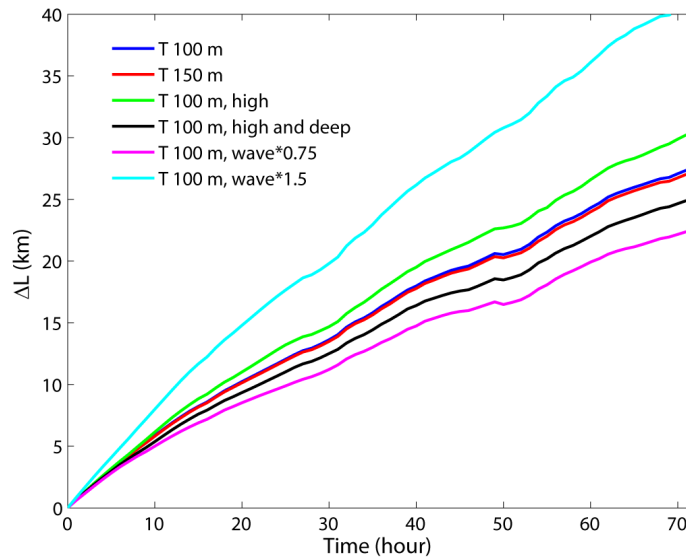


Figure 3.12: The “ensemble” mean deviation in the experiments for various parameters.

3.4 Velocity frequency

One important aspect of the model performance is how quickly the icebergs move. This is also an important factor in any risk analysis of icebergs (Korsnes & Moe, 1994; Zubakin et al., 2005). To investigate this quantity we compute the distribution of how many km that the icebergs move in 1 hour. The results from the observations and model are shown in Fig. 3.13. We notice that there is a good agreement between observations and the model, and we conclude that the model displays the correct order of magnitude velocity field. This is in agreement with the visual interpretation of the trajectory plots in Sec. 3.2. It should be noted that the validation of the underlying ocean current also showed good statistics on the velocity distribution at available current rigs confirming this observation (Broström et al., 2009).

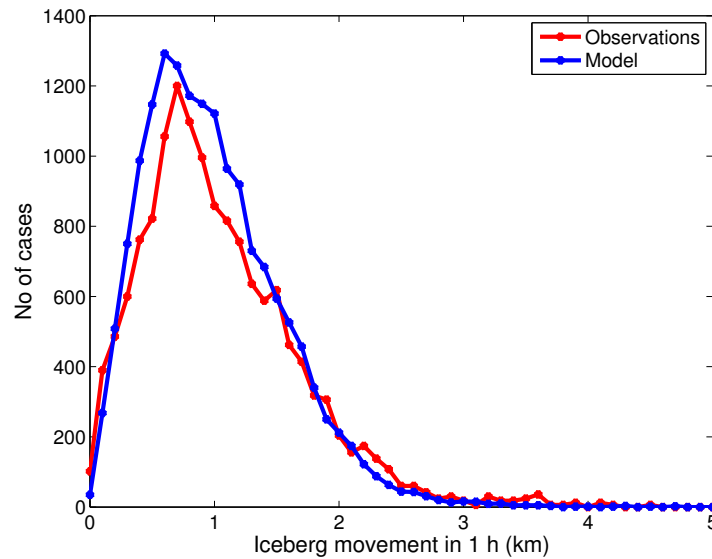


Figure 3.13: The frequency distribution of how far an iceberg moves during one hour. Data from IDAP and the iceberg model are shown in the figure. The interval count is 0.1 km.

3.5 Deterioration

There are no detailed data available to check the deterioration of the model. Nevertheless, we plot the size of the iceberg as a function of time in Fig. 3.14, the initial size in this experiment is always 100 m. We see that the iceberg size drops by about 5 m in the course of 3 days. If the melt rate were to be constant it would imply that a 100 m tabular iceberg would melt in 60 days, but a small iceberg melts quicker than a large iceberg (the decline in size of a 75 m iceberg over 3 days is about 7 m). Hence, we may conclude that the 100 m iceberg would probably melt in less than, say, 40-50 days (see also Broström et al., 2009). We know that the Argos transmitters on the icebergs survived for more than 50 days in most circumstances, and well into the summer in some case. However, we do not know the initial size if the icebergs; on one side there were few very large icebergs reported from the area, on the other side perhaps the largest icebergs were selected for mounting the Argos tracking system. This represents an unknown and we can make no conclusive statement on the deterioration rate but we want to flag that the melting rate seems suspiciously high: furthermore, the evaluation of the hindcast data indicated that the modeled temperature may be slightly too warm (Broström et al., 2009). An iceberg with a size of 200 m will probably survive at least 150 day.

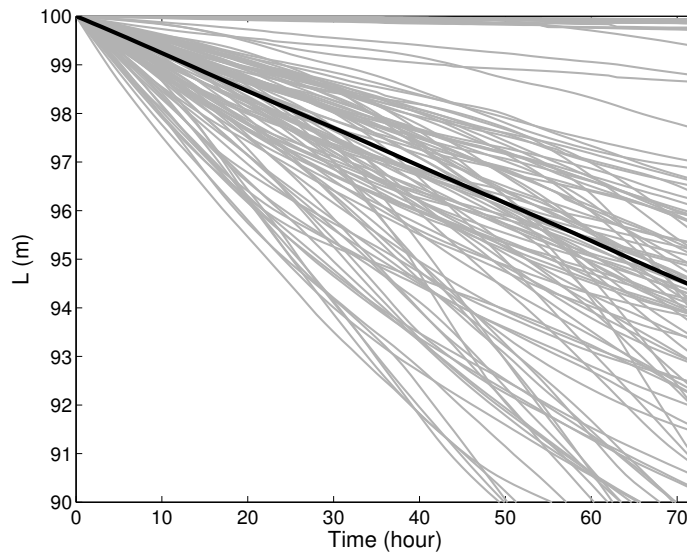


Figure 3.14: The iceberg size as a function of time for the 72h hindcasts made in this study.

Note that all hindcasts were started with a tabular iceberg size of 100 m.

The melting due to the various processes described in Sec. 2.3 is shown in Fig. 3.15. We see that swell waves and wind waves are the most important processes for iceberg deterioration in the present set of experiments. The forced convection in water and air are also significant. Somewhat surprising is that the calving is almost negligible, but it may be due to the relatively short hindcasts in combination with the large size of the icebergs. However, the results are well within the uncertainties of the strength of the different deterioration processes as outlined in the first part of Sec. 2.2 (Savage, 1999). The impact of solar radiation was almost negligible in this study (not shown).

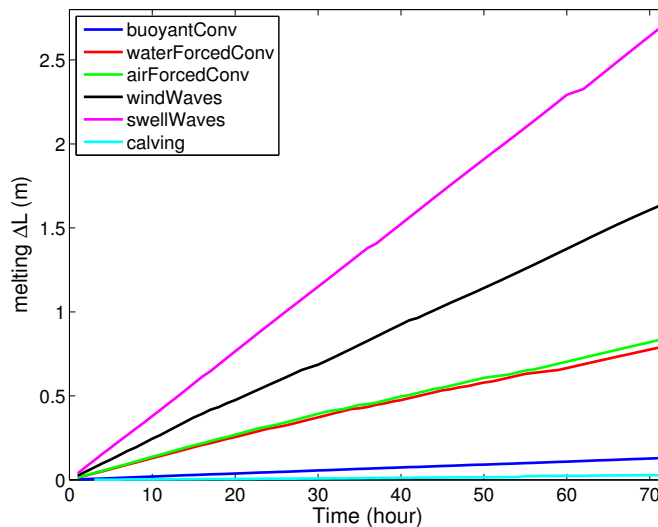


Figure 3.15: The iceberg melting due to various processes as a function of time for the hindcasts made in this study. Note that all hindcasts were started with a tabular iceberg size of 100 m.

4 Results and discussion

This report presents results from a verification and validation study of the CHC iceberg model (Kubat et al., 2007; Kubat et al., 2005), and its implementation in the met.no modeling system for the Barents Sea. It is demonstrated that the model code works well and is consistent with the forcing fields generated at met.no. The iceberg model is forced with atmospheric wind, oceanic currents and temperature, ice coverage, ice thickness, ice speed and direction, and wave radiation stress. All these data have been reanalyzed for the study period and are available from August 1987 to August 1988. More details on the hindcast data can be found in Broström et al. (2009). Data from iceberg movements recorded during the IDAP program (Løset & Carstens, 1996; Spring, 1994) and the hindcast for icebergs during this period are studied in some detail in Section 3.

For the iceberg drift, the ocean current, and the ice drift in the presence of ice, are the most important factors followed by the wave radiation stress. Wind forcing is the least important factor. This is consistent with previous results (Kubat et al., 2007; Kubat et al., 2005; Savage, 1999; Savage, 2001). The mass (or geometry) of the iceberg may also be an important factor under some conditions. However, for tabular icebergs which keep their keel depth during deterioration in the present model formulation⁹, melting is not particularly important for the simulated path. We conclude that as far as the iceberg drift is concerned, deterioration processes is most important for relatively small pinnacle icebergs.

The performance of the model is good, especially given the uncertainties in the geometrical shape of the iceberg. The model velocity statistics is very good, showing the capability of the model for risk assessments. The performance of the long term advection of icebergs from key source regions, and some overall discussion on deterioration processes, are briefly discussed in the report on the hindcast data validation (Broström et al. 2009).

4.1 Possible model improvements

There are of course many simplifications involved in designing an iceberg drift model for operational use. It should be highlighted that the model formulation is robust and covers the most important aspects of the iceberg drift and deterioration. Furthermore, the iceberg model is based on simple parameterizations based on observations such that a reformulation of the model to a more realistic formulation may require considerable work and testing. Nevertheless, there are some possible weak points in the present model formulation that we want to point out.

- The iceberg geometry may have to be adjusted for the Barents Sea, given the observed relations between characteristic iceberg length and iceberg height. The iceberg depth remains largely unknown at the present stage.
- One potential problem in the deterioration module is that the melting depends on the surface temperature alone. In reality, the total temperature profile will be important; however, the present formulation reflects the total uncertainties within the entire model formulation and is based on observations (Kubat et al., 2007). In the present formulation icebergs do not melt in ice water (i.e., surface water at the

⁹ Note that the main deterioration is at the sides of the icebergs such that rectangular tabular icebergs will remain essentially rectangular.

freezing point) albeit there may be warm water present at some depth underneath the ice.

- The stratification of the ocean may be important for introducing internal wave drag on deep icebergs. This is not included in the present model; however, the relative strength of this factor should be estimated before making any final statement on its importance for the present model.
- The wave radiation stress is presently divided into a swell part where direction is taken from the wave model and a wind-wave part assumed to be in the direction of the wind. The present formulation based on a wave model may benefit from taking the entire wave forcing from the wave model.
- The model is designed for large icebergs, and the characteristic size of icebergs should be at least 20-50 m. For small icebergs, at least the following processes will need adjustment
 - The wave radiation stress may be different for small icebergs than for large icebergs (small icebergs move with the wave while large icebergs reflect the wave).
 - Small icebergs will start to move vertically due to wave motion and this may enhance the melting of the iceberg.
- In the present model formulation, the small iceberg bits and growlers produced in the calving process are not described. There are formulations describing the statistical distribution during the calving process (Savage et al., 2000). It is possible to consider a model development where such forcing functions (or statistical release of small icebergs and ice rocks from the mother iceberg) can be combined with statistical formulations of the movement of Lagrangian particles (LaCasce, 2008) to determine a statistical map for the risk of encountering a iceberg bit of a certain size around the iceberg. It should be noted that the melting rate of the small iceberg bits must be well described in such a statistical model (Savage et al., 2000).

Acknowledgement

Kenneth Johannessen at StatoilHydro provided the data from the IDAP study. Furthermore, he gave very valuable comments on an early version of this report.

References

- Abramov, V.A., 1992: Russian iceberg observations in the Barents Sea 1933-1990. *Polar Research* 11, 93-97.
- Albretsen, J. & I. Burud, 2006: Assimilation of sea surface temperature and sea ice concentration in a coupled sea ice and ocean model. In: H. Dahlin, N.C. Flemming, P. Marchand and S.E. Petersson (Editors), *European Operational Oceanography: Present and Future*. 4th International Conference on EuroGOOS, Brest, France, pp. 663-668.
- Barker, A., M. Sayed & T. Carrieres, 2004: Determination of Iceberg Draft, Mass and Cross-Sectional Areas, 14th Internat. & Offshore Polar Eng. Conf., ISOPE, Toulon, France.
- Broström, G. & K. Christensen, 2008: Waves in ice. Research report, 5, Norwegian Meteorological Institute, Oslo, Norway. pp. 68.
- Broström, G., A. Melsom & A. Carrasco, 2009: Iceberg modelling at met.no: evaluation of hindcast study. Report series, 16, Norwegian Meteorological Institute, Oslo, Norway. pp. 63.
- Cavaleri, L., *et al.*, 2007: Wave modelling - The state of the art. *Progress in Oceanography* 75, 603-674.
- Engedahl, H., 1995: Implementation of the Princeton Ocean Model (POM/ECOM3D) at the Norwegian Meteorological Institute. Research Report, 5, Norwegian Meteorological Institute, Oslo, Norway.
- Flather, R.A., 1981: Results from a model of the north-east Atlantic relating to the Norwegian coastal current. In: R. Sætre and M. Mork (Editors), *The Norwegian Coastal Current: Vol II*. University of Bergen, Bergen, Norway, pp. 427-458.
- Gjevik, B., E. Nost & T. Straume, T., 1990: Atlas of tides on the shelves of the Norwegian and the Barents Sea. Rep., Department of Mathematics, University of Oslo, Oslo, Norway.
- Gjevik, B., E. Nøst & T. Straume, 1994: Model simulations of the tides in the Barents Sea. *Journal of Geophysical Research* 99, 3337-3350.
- Komen, G.J., L. Cavaleri, M. Donelan, K. Hasselmann, S. Hasselmann and coauthors, 1994: *Dynamics and modelling of ocean waves*. Cambridge University Press, Cambridge, 532 pp.
- Korsnes, R. & G. Moe, 1994: Approaches to find iceberg collision risks for fixed offshore platforms. *International Journal of Offshore and Polar Engineering* 4, 48.
- Kubat, I., M. Sayed, S.B. Savage, T. Carrieres & G. Crocker, 2007: An operational iceberg deterioration model, 17th International Offshore and Polar Engineering Conference.
- Kubat, I., M. Sayed, S.B. Savage & T. Carriers, 2005: An operational model of iceberg drift. *International Journal of Offshore and Polar Engineering* 15, 125-131.
- LaCasce, J.H., 2000: Float and f/H. *Journal of Marine Research* 58, 61-95.
- LaCasce, J.H., 2008: Statistics from Lagrangian observations. *Progress in Oceanography* 77, 1-29.

- Lichey, C. & H.H. Hellmer, 2001: Modeling giant-iceberg drift under the influence of sea ice in the Weddell Sea, Antarctica. *Journal of Glaciology* 47, 452-460.
- Longuet-Higgins, M.S., 1977: The mean forces exerted by waves on floating or submerged bodies with application to sand bars and wave power machines. *Proceedings of Royal Society London, Series A* 352, 463-480.
- Løset, S., 1993: Numerical modeling of the temperature distribution in tabular icebergs. *Cold Regions Science and technology* 21, 103-115.
- Løset, S. & T. Carstens, 1996: Sea ice and iceberg observations in the western Barents Sea in 1987. *Cold Regions Science and Technology* 24, 323-340.
- Neshyba, S. & E.G. Josberg, 1980: On the estimates of Antarctic iceberg melt rate. *Journal of Physical Oceanography* 10, 1681-1685.
- Nøst, O.A. & P.E. Isachsen, 2003: The large-scale time-mean ocean circulation in the Nordic Seas and Arctic Ocean estimated from simplified dynamics. *Journal of Marine Research* 61, 175-210.
- Pite, H.D., D.R. Topham & B.J. van Hardenberg, 1995: Laboratory measurements of the drag force on a family of two-dimensional ice keel models in an two-layer flow. *Journal of Physical Oceanography* 25, 3008-3031.
- Røed, L.P. & J. Debernard, 2004: Description of an integrated flux and sea-ice model suitable for coupling to an ocean and atmosphere model. *Research Report, 4*, Norwegian Meteorological Institute, Oslo, Norway. pp. 51.
- Savage, S.B., 1999: Analyses for Iceberg Drift and Deterioration Code Development. *Technical Report Canadian Ice Service*. pp. 50.
- Savage, S.B., 2001: Aspects of iceberg deterioration and drift. In: N.J. Balmforth and P. A. (Editors), *Lecture Notes in Physics Series: Geomorphological Fluid Mechanics*. Springer-Verlag, Berlin, pp. 279-318.
- Savage, S.B., 2007: Modelling wave radiation stress in the CIS iceberg drift and deterioration program. report to Canadian Hydraulic Centre.
- Savage, S.B., 2008: Sea ice forces on icebergs. Canadian Hydraulic Institute.
- Savage, S.B., G. Crocker, M. Sayed & T. Carrieres, 2000: Size distribution of small ice pieces calved from icebergs. *Cold Regions Science and Technology* 31, 163-172.
- Sayed, M., 2008: Code documentation of iceberg drift and deterioration model. Canadian Hydraulic Institute.
- Spring, W., 1994: Ice data acquisition program (IDAP) summary report. Dallas E&P Engineering: Dallas. pp. 90.
- Squire, V.A., 2007: Of ocean waves and sea-ice revisited. *Cold Regions Science and technology* 49, 110-133.
- Squire, V.A., J.P. Dugan, P. Wadhams, P.J. Rottier & A.K. Liu, 1995: Of ocean waves and sea-ice. *Annual Review of Fluid Mechanics* 27, 115-168.
- Undén, P., L. Rontu, H. Järvinen, P. Lynch, J. Calvo and coauthors, 2002: HIRLAM-5 Scientific Documentation. Swedish Meteorological and Hydrological Institute,

Norrköping, Sweden.

- Wadhams, P., 2000: Ice in the ocean. Gordon and Breach science publisher, London, 351 pp.
- Walín, G., 1972: On the hydrographic response to transient meteorological disturbances. *Tellus* 24, 1-18.
- White, F.M., M.L. Spaulding & L. Gominho, 1980: Theoretical estimates of the various mechanisms involved in iceberg deterioration in the open ocean environment. U.S. Coast Guard., Washington, D.C. pp. 126.
- Zubakin, G.K., A.K. Naumov & I.V. Buzin, 2004: Estimates of ice and iceberg spreading in the Barents Sea, 14th International Offshore and Polar Engineering Conference, Toulon, France, pp. 863-870.
- Zubakin, G.K., A.G. Shelomentsev, D.K. Onshuus, L.I. Eide & I.V. Buzin, 2005: Spatial distribution of icebergs in the Barents Sea based on archived data and observations of 2003, 18th International Conference on Port and Ocean Engineering (POAC-2005). "Arctic-Shelf" Laboratory, Arctic and Antarctic Research Institute, St. Petersburg, Russia, Potsdam, USA, pp. 575-583.